We report here experiments in which pressures of 1 Mbar were reached, as measured by a further extension of the new NBS scale. The data are reproducible and can be easily compared with other types of calibration. The estimated uncertainty in pressure is no greater than 10 percent. To the best of our knowledge, this is the highest static pressure ever reached in an experiment in which an internal calibration was employed.

The difference between external and internal calibration of pressure is fundamental. External procedures usually involve monitoring mechanical loading of high-pressure apparatus. However, the loading is not transmitted to an internal sample because the apparatus deforms, and as parts begin to yield it is not possible to determine the internal pressure.

In the experiments reported here, it was possible to monitor the sample being pressurized with a new diamond-windowed cell. The cell was designed for static experimentation in the megabar pressure range, which was inaccessible with previous apparatus. Ruby fluorescence in the cell was excited by a laser beam, and its wavelength was monitored continuously with a spectrometer linked to the pressure cell by a fiber optic bundle.

The improved diamond pressure cell used in the experiments has been described in detail by Mao and Bell (*6*) and is shown diagrammatically in Fig. 1. The apparatus consists of two single-crystal diamonds opposed as pressure anvils. A scissors-shaped lever-block assembly is spring-loaded to apply a mechanical advantage of 2. The diamonds are supported by half-cylinder seats of tungsten carbide with a zirconium shim (0.001 inch thick) placed between the low-pressure-bearing surfaces. The half-cylinders are adjusted to achieve and maintain excellent alignment of the diamonds (to better than one-half a Newton color fringe interference of the diamond faces) during an experiment. A sheet (0.010 inch thick) of work-hardened steel (*7*) is placed between the high-pressure diamond faces, and then a crystal of ruby is placed on the steel and pressed into it as the diamond anvils are squeezed together. Blue laser light (*8*), wavelength 441 nm, is used to excite fluorescence in the ruby. Spectrometer and detector systems are the same as previously described (*6*), except that the photomultiplier tube in the experiments was cooled to –50°C to reduce dark noise (*9*).

Before the experiments were done we observed the sodium chloride B1–B2 (NaCl-CsCl structure types) transition at 291 kbar (*1*) and simultaneously measured the wavelength of the R_1 ruby line. A single ruby fragment was monitored each time an experiment was done. The observed spectral shift of the R_1 ruby line in a typical experiment and the corresponding pressures from a linear extension of the NBS scale are listed in Table 1. The intensity of the R_1 ruby line appeared to diminish slightly as the pressure was increased to the megabar range. No sign of mechanical failure was observed in the diamonds, and with improved support it should be possible to increase the pressure to at least 1.5 Mbar.

Table 1. Observed spectral shift ($\Delta\lambda$) of the R_1 line of a ruby crystal at high pressure. The shift of 106 Å (values in italics) corresponds to the B1–B2 transition in NaCl. Pressures below 291 kbar were determined from the NBS calibration curve (*2*). Pressures above 291 kbar were determined from a linear extension of the NBS curve.

$\Delta\lambda$ (Å)	Pressure (kbar)
30	83
75	206
106	*291*
180	495
225	619
290	797
310	823
320	880
370	1018

The capability of routinely experimenting at pressures in the megabar range has far-reaching applications. It will be possible to study insulator-metal transitions and numerous other proposed physical and chemical changes in materials at high pressures (*10*). The accessibility of this pressure range coupled with the high temperatures already reached (*2*) makes it possible to experiment directly at the conditions of the earth's core.

H. K. Mao
P. M. Bell

Geophysical Laboratory,
Carnegie Institution of Washington,
Washington, D.C. 20008

References and Notes

1. G. J. Piermarini and S. Block, *Rev. Sci. Instrum.* **46**, 973 (1975).
2. P. M. Bell and H. K. Mao, *Carnegie Inst. Washington Yearb.* **74**, 399 (1975).
3. G. J. Piermarini, S. Block, J. O. Barnett, R. A. Forman, *J. Appl. Phys.* **46**, 2774 (1975).
4. H. G. Drickamer, *Rev. Sci. Instrum.* **41**, 1667 (1970).
5. N. Kawai and S. Mochizuki, *Phys. Lett. A* **36**, 54 (1971).
6. H. K. Mao and P. M. Bell, *Carnegie Inst. Washington Yearb.* **74**, 402 (1975).
7. This material was kindly supplied by L. C. Ming, University of Rochester.
8. Meterologic Instruments, Inc., Bellmawr, N.J., He-Cd laser ML 442.
9. Products For Research Inc., Danvers, Mass., Carnot-cycle cooler.
10. P. M. Bell and H. K. Mao, *Carnegie Inst. Washington Yearb.* **73**, 507 (1974).

11. We wish to thank G. J. Piermarini and S. Block of the National Bureau of Standards and A. Van Valkenburg of the Geophysical Laboratory for useful suggestions and assistance in this project.

29 December 1975; revised 8 January 1976

Surface Predominance of Trace Elements in Airborne Particles

Abstract. *A number of minor and trace elements including Be, C, Ca, Cr, K, Li, Mn, Na, P, Pb, S, Tl, V, and Zn present in coal fly ash are found to be preferentially concentrated on the particle surfaces. Environmentally effective concentrations of these elements are thus much higher than indicated by conventional bulk analyses.*

It is now well established that toxic trace elements such as As, Be, Cd, Cr, Mn, Ni, Pb, Sb, Se, Tl, V, and Zn are being mobilized in the atmosphere in association with particles emitted from fossil fuel combustion and conversion (*1*). It has also been shown (*1–3*) that the specific concentrations of many of these elements (in micrograms per gram of fly ash) increase with decreasing particle size in fly ash derived from coal combustion. Consequently, the highest trace element concentrations are encountered in small particles which most readily pass through control devices, which remain suspended in the atmosphere for long periods, and which deposit in the innermost regions of the human respiratory tract when inhaled (*2, 4*).

Recently, it has been suggested (*5*) that this dependence of elemental concentration on particle size occurs because certain elements (or their compounds) are volatilized in the high-temperature coal combustion zone and then condense uniformly onto the surfaces of entrained fly ash particles as the temperature falls. Such surface deposition would give rise to the observed inverse dependence of specific concentration on the diameter of the approximately spherical fly ash particles (*2, 3*).

If surface deposition does occur, either as a result of the postulated mechanism or otherwise, then the actual concentrations of toxic material present at the point of contact of a particle with living tissues may be substantially higher than hitherto supposed on the basis of bulk analyses. To establish whether the surface concentrations of toxic elements are higher, we have determined the dependences of several elemental concentrations as a function of depth in individual coal fly ash particles.

The fly ash samples studied were collected in the stack systems of two coal-fired power plants burning midwestern U.S. bituminous coals. One plant was of small capacity and obsolete design utilizing a chain grate stoker; the other was a large modern plant with an input of pulverized coal.

Since surface deposition implies that elemental concentration per unit surface area should be independent of particle diameter, large particles (75 to 100 μm) were studied for convenience. These particles were pressed into In foil and mounted in the specimen chamber of an ion microprobe (AEI model IM 20). A 35-kev negative oxygen ion beam 80 na in intensity and about 16 μm in cross-sectional diameter was then rastered rapidly over an area 100 by 100 μm enclosing the particle being studied. Sputtering rates were estimated within about a factor of 2 by comparison with measured rates for pure Si samples at the same current density.

Using mass spectrometer resolutions ranging up to 4000, we identified the elements listed in Table 1 in the sputtered material. Bulk concentrations of these elements, as determined by spark source mass spectrometry, are also listed in Table 1. Additional elements present could not be uniquely identified by ion microprobe mass spectrometry, either because of interferences from molecular and multiply charged ions or because of inadequate detection capability. We determined the elemental abundance as a function of sputtering time (and thus depth) both by monitoring the mass spectral intensity of a single element continuously utilizing electrical detection and by simultaneously recording complete mass spectra photographically at different sputtering times.

Table 1. Surface predominance of elements in fly ash particles; I_s/I_{500}, signal intensity at the surface divided by the signal intensity at a depth of 500 Å.

Element	Bulk concentration* (μg/g)	I_s/I_{500}	Technique†
	Matrix elements		
Al	>>15,500	1.1	a, b, c
Fe	92,400	0.7	a, b, c
Si	110,000	1.1	a, b, c
	Minor elements		
C		3.5	a, b
Ca	>28,600	1.6‡	a, b, c
K	38,800	7.6	a, b, c
Mg	12,300	0.9	a
Na	>19,700	15.2	a, b, c
P	600	3.8	a, c
S	7,100	7.7	a, b, c
Ti	4,740	0.9	a
	Trace elements		
Be	32	6.0	a
Cr	380	3.3	a, c
Li	200	3.8	a
Mn	310	6.4	a
Pb	620	11.0	a, c
Tl	28	10.0	a
V	380	2.0	a
Zn	1,250	7.2	a, c

*Determined by spark source mass spectrometry. †a, Secondary ion mass spectrometry; b, Auger electron spectrometry; c, electron-induced x-ray spectrometry. ‡Only samples derived from some sources exhibited surface predominance.

As predicted, a number of elements exhibit a significant increase in concentration near particle surfaces (Table 1). Some representative depth profiles are presented in Fig. 1 for the matrix elements Fe and Si, the toxic trace elements Pb and Tl, and the minor constituent K. These depth profiles are presented in arbitrary units of secondary ion intensity since each element was recorded under different conditions of gain and mass resolution. The relative scales are, however, considered to be linear.

Corroborative evidence was obtained from both Auger microprobe and electron microprobe studies. The Auger microprobe detects only elements present within 10 to 20 Å of the surface, and we obtained depth profiles by sequentially etching approximately 10 Å of the surface away with a beam of Ar^+ ions. Because of charging effects and lack of sensitivity, we were able to detect only Al, C, Ca, Fe, K, Na, S, and Si by Auger electron spectrometry (Table 1); however, depth profiles for these elements very similar to those obtained with the use of ion microprobe mass spectrometry were observed. The electron microprobe detects elements present within 1 to 2 μm of the particle surface. We prepared samples for analysis by first etching several thousand angstroms of material off one side of each particle with an Ar^+ milling apparatus. Comparison of the normalized x-ray spectra obtained from a particle surface and from its interior indicated the surface predominance of Cr, K, Na, P, Pb, S, and Zn (Table 1).

In order to reduce the possibility that these depth dependences might be due to instrumental, sputtering, or sample artifacts, In foil mountings and some pure metallic oxide particles (for example, PbO_2) were profiled and shown not to exhibit any elemental surface predominance. In addition, a number of fly ash particles derived from different power plants were shown to exhibit remarkably similar depth profiles. The possibility of artifacts arising from differential sputtering or from chemical effects due to oxygen implantation cannot be completely eliminated but seems unlikely in view of the agreement obtained from three fundamentally different analytical approaches.

Semiquantitative estimates of the ratio of the surface concentration to the interior concentration for matrix and minor elements can be obtained directly from ion microprobe and Auger microprobe depth profile data. Some representative results, for which signal intensities obtained at an arbitrary depth of 500 Å are used to represent interior concentrations, are listed in Table 1. It is, however, difficult to estimate similar concentration ratios for trace elements because of substantial contributions to the mass spectral base line by interfering ions. The ratios listed in Table 1 for trace elements should therefore be considered as minimum values. However, the spectral background immediately surrounding the Pb and Tl isotopes can be estimated since the absence of large concentrations of interfering ions with high mass gives rise to a relatively uniform background ion intensity. With this correction the ratios obtained were 30 and 50, respectively. These results are in substantial agreement with the results of ion microprobe analyses in which glass standards containing Pb and Tl were used for calibration purposes and which indicated Pb and Tl concentrations of the order of 1 percent within 100 Å of the particle surfaces.

Although these findings undoubtedly support the idea that volatile elements con-

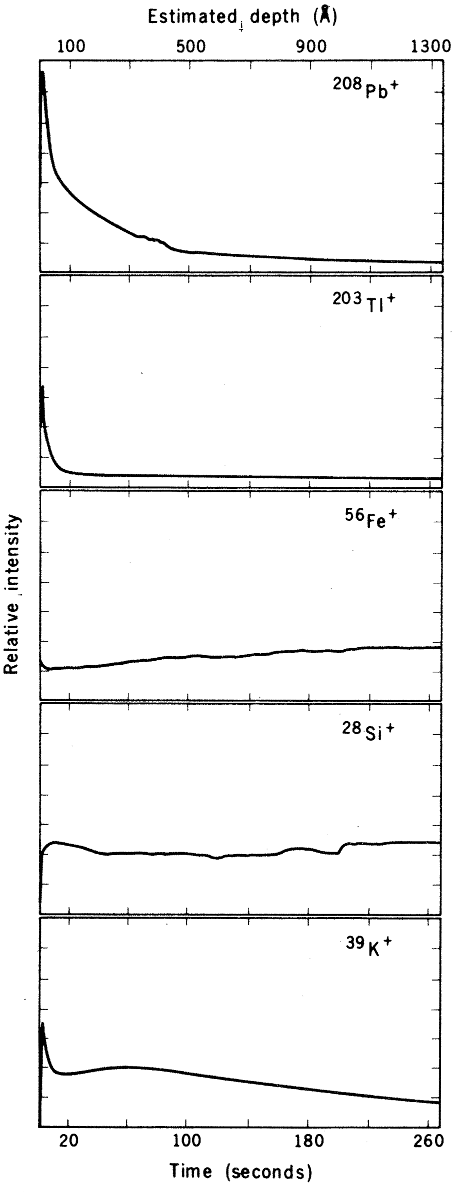

Fig. 1. Relative concentrations of Pb, Tl, Fe, Si, and K as a function of depth in individual fly ash particles as determined by ion microprobe mass spectrometry.

dense onto the surface of fly ash particles during, or soon after, coal combustion, alternative mechanisms, such as the diffusion of certain species to the surface of molten particles, cannot be excluded. It seems probable, however, that the surface predominance of certain elements is a widespread phenomenon in particles derived from high-temperature processes since preliminary studies have established its occurrence for Br, Cl, and Pb in automobile exhaust particulates and for Mn and Zn in fly ash from a municipal incinerator.

These results are of real significance because they show that conventional bulk analyses provide a poor measure of the actual concentrations of many toxic trace elements that are in effective contact with the external environment of a particle. In the case of fly ash, whose matrix consists primarily of an insoluble aluminosilicate glass, it is appropriate to think in terms of an accessible or extractable shell at the particle surface with which body fluids, water, or reactant species can interact. Initial studies indicate that elements extractable from fly ash by water and by dimethyl sulfoxide are derived from within a shell approximately 1000 Å in depth below the external particle surface, and it seems probable that this shell corresponds to the region of surface enhancement discussed here. For the large (75 to 100 μm) particles studied, only a small fraction of the content of a given trace element may be present in the surface layer; however, for a particle with an aerodynamic diameter of 1 μm as much as 80 percent of the trace elemental mass is apparently in this layer (*2*). This point should be recognized in the design of realistic bioassay or inhalation studies involving simulated particles.

R. W. LINTON, A. LOH
D. F. S. NATUSCH*
School of Chemical Sciences,
University of Illinois, Urbana 61801
C. A. EVANS, JR., P. WILLIAMS
Materials Research Laboratory,
University of Illinois

References and Notes

1. R. E. Lee, Jr., and D. J. von Lehmden, *J. Air Pollut. Control Assoc.* **23**, 853 (1973); R. E. Lee, Jr., S. S. Goranson, R. E. Enrione, G. B. Morgan, *Environ. Sci. Technol.* **6**, 1025 (1972); H. A. Schroeder, *Environment* **13**, 18 (1971).
2. R. L. Davison, D. F. S. Natusch, J. R. Wallace, C. A. Evans, Jr., *Environ. Sci. Technol.* **8**, 1107 (1974).
3. J. W. Kaakinen, R. M. Jorden, M. H. Lawasani, R. E. West, *ibid.* **9**, 862 (1975).
4. D. F. S. Natusch and J. R. Wallace, *Science* **186**, 695 (1974).
5. → ——, C. A. Evans, Jr., *ibid.* **183**, 202 (1974).
6. This work was supported in part by NSF grants ERT-74-24276, MPS-74-05745, and DMR-72-03026. R. W. L. is the recipient of an NSF Energy Related Graduate traineeship and A.L. of a fellowship from the Granite City Steel Company.

* Present address: Department of Chemistry, Colorado State University, Fort Collins 80523.

30 July 1975; revised 18 November 1975

Reproductive and Vegetative Morphology of a Cretaceous Angiosperm

Abstract. *Recent collections from plant-bearing deposits of Cenomanian age in central Kansas have yielded angiosperm axes with helically arranged, seed-bearing, conduplicate carpels. Large leaves associated with these fruits are thought to represent parts of the same kind of plant because the leaves and fruits are the only plant fossils at this locality to have distinctive, morphologically identical, yellow bodies within their carbonaceous remains. These fossils provide a rare opportunity to study the morphology of an ancient angiosperm and illustrate the antiquity of certain features considered primitive by comparative angiosperm morphologists.*

The uncertain nature of the structure of early angiosperms has been the major impediment to understanding the origin and early evolutionary radiation of this important plant group. The earliest evidences of angiospermy in the fossil record are Lower Cretaceous pollen (*1*) and leaf impressions (*2*). Reports of angiosperm reproductive structures of Cretaceous age are not common and, when published, almost never include much morphological or structural detail. As a result, the present concepts of primitive floral features have been determined with little reference to the fossil record.

Deposits of plant-bearing clays have recently been found in the Janssen Clay Member of the Dakota Formation. These clays occur in northeast Russell County, Kansas, and underlie the Rocktown Channel sandstone in that area. Siemers (*3*), in a detailed study of the Cretaceous sediments of Russell County, assigns the Janssen Clay Member to the lowermost Cenomanian and uppermost Albian. Examination of the pollen and spores from the Janssen Clay Member also suggests a lowermost Cenomanian age (*4*).

A diverse assemblage of impressions and well-preserved compressions of angiosperm leaves and reproductive structures, gymnosperm foliage, and ferns has been collected from this clay. The plants are similar to those reported earlier by Lesquereux (*5, 6*) from the Dakota Formation and by Newberry (*7*) from the Amboy Clays of the Raritan Formation of New Jersey. One interesting component of this fossil flora is an angiospermous reproductive axis, which is well enough preserved to allow detailed study of its morphology (*8*).

The reproductive axis is elongate (axes up to 12 cm in length have been discovered; although none were complete) and bears more than 50 helically arranged conduplicate carpels (Fig. 1d). These are elongate, flattened laterally, enlarge gradually from a proximal stalk, and terminate in a narrow rounded tip (Fig. 2). The abaxial surface is rounded, and a suture extends the length of the adaxial surface of the carpel. The adaxial suture is bounded on either side by extensions of the carpel walls, which fold outward about 5 mm, forming an adaxial crest (Fig. 1c). No separate stigmatic surface has been observed, and it is possible that the recurved carpel walls may have served this function.

The carpels are attached to the axes by stalks 1 mm wide and 7 mm long, which have decurrent bases (Fig. 2). A distinctive feature of these stalks is a shallow groove about midway between the carpel and the point of attachment. Since carpels found dispersed in the matrix never have such a groove on their stalks, and the stalks of these dispersed carpels are about 2.5 to 3 mm long, the length that would be expected if they separated at this point, it is assumed that this groove represents a point of abscission. Isolated carpels, open at the adaxial suture and filled with clay, are also found preserved as casts and molds. The fruit is a follicle.

Compressions and impressions of the carpels often have a partitioned appearance due to a line of depressions in the adaxial two-thirds of the carpel (Figs. 1d and 2). Occasionally, what appear to be small compressed seeds can be observed in these depressions (Fig. 1a). These are small (1.4 by 0.6 mm) and their position suggests that the placentation is submarginal. When carbonaceous material is removed from the area where compressed seeds occur and is cleared, the remains of seed coats can be isolated (Fig. 1b). The size of these agrees with that of the compressed seeds recovered in situ.

No pollen-bearing organs, calyx, or corolla is associated with the carpels or the elongated axes. No complete axis was found, so we cannot speculate on the possible association of these various organs with these axes.

Small (40 to 50 μm in diameter) yellow bodies are commonly distributed over much of the surface of the compressed carpels. Although these bodies may be lost in collecting or preparation, they often leave definite punctate surfaces. Similar yellow bodies are also a common feature in the mesophyll of *Liriophyllum*, one of the leaves found in the same sediments (Fig. 1, e and f), but are not found in any other plant fossils from this locality. The mor-